Results from the GPS Flight Experiment on the High Earth Orbit AMSAT OSCAR-40 Spacecraft

Michael C. Moreau, Edward P. Davis, J. Russell Carpenter
NASA Goddard Space Flight Center

David Kelbel, *Computer Sciences Corporation*

George W. Davis, *Emergent Space Technologies*

Penina Axelrad, *University of Colorado at Boulder*

ABSTRACT

A GPS receiver flying on the High Earth Orbit (HEO) AMSAT-OSCAR 40 (AO-40) spacecraft has been returning GPS observations from high above the altitude of the GPS constellation. AO-40, an amateur radio satellite launched November 16, 2000, is currently in a low inclination, 1000 by 59000 km altitude orbit. This low-cost experiment utilizes a mid 1990's era, 6-channel, C/A code receiver configured with high gain receiving antennas for tracking above the GPS constellation. The receiver has performed well, despite operating significantly outside of its original design environment. It has regularly returned GPS observations from points all around the orbit, with over ten weeks of GPS tracking data collected to date. Signal to noise levels as high as 48 dB-Hz have been recorded near apogee, when the spacecraft was at an altitude of close to 60000 km. GPS side lobe signals have been tracked on several occasions, primarily from Block IIR GPS satellites. Although the receiver has not computed a solution in real-time, point solutions have been computed on the ground using simultaneous measurements from four satellites. This experiment has provided important experience dealing with the many challenges inherent to GPS tracking at high altitudes, and the measurements returned are providing valuable information about the characteristics of GPS signals available for future HEO users.

INTRODUCTION

The AMSAT OSCAR-40 (AO-40) satellite is the latest in a series of low-cost spacecraft built by the Radio Amateur Satellite Corporation (AMSAT), designed for radio amateurs to experience satellite tracking and to participate in radio propagation experiments. AO-40, easily the largest, most sophisticated amateur radio satellite to date, was launched November 16, 2000 aboard an Ariane 5 from Kourou, French Guiana.

Figure 1: AO-40 spacecraft in Kourou.

The flight of a GPS receiver on the AO-40 spacecraft was conceived in the mid-1990s as a low cost experiment to demonstrate the feasibility of tracking GPS signals in a High Earth Orbit (HEO) utilizing existing receiver technology [1]. The experimental team included personnel from AMSAT and NASA GSFC. The original goals for the GPS experiment included demonstrating the operation of a GPS receiver in a HEO without requiring interaction from ground controllers; returning signal level measurements to map the GPS satellite antenna patterns above the constellation; and generating orbit and attitude solutions for the AO-40 spacecraft for operational use. The GPS experiment was first activated in September, 2001.

Several flight experiments in which GPS receivers were operated in HEOs took place before the launch of AO-40. In 1997, TEAMSAT [2] and EQUATOR-S [3] demonstrated closed-loop tracking of GPS signals from above the GPS constellation, including measurements recorded at altitudes exceeding 60000 km, and tracking of side lobe signals. That same year, the Falcon Gold satellite successfully recorded GPS signals from within a geostationary transfer orbit using a low power digital sampling receiver [4]. In 2000, the first public disclosure was made regarding the successful demonstration of a GPS-based orbit determination system on a restricted US Department of Defense satellite in a geostationary orbit [5]. In spite of these achievements, only a limited amount of high altitude GPS data has been returned and is available to civilian users. The results from AO-40 help to fill in some gaps in our understanding of the actual signal characteristics for future high altitude GPS users.

This paper provides a description of the AO-40 spacecraft and design of the GPS experiment, followed by an overview of the significant results and lessons learned from the experiment to date. The subsequent sections go into greater detail regarding tracking performance, measured power levels from the GPS satellites, and the latest orbit determination analysis.

AO-40 SPACECRAFT, ORBIT, AND GPS EXPERIMENT

The AO-40 spacecraft was originally intended to achieve a Molniya orbit, but after an "incident" with the propulsion system that nearly resulted in loss of the spacecraft in December 2000, remaining fuel was used to insert into the stable, low inclination, elliptical orbit described in Table 1 and illustrated in Figure 2 [8]. The AO-40 spacecraft is currently spin-stabilized about the body Z-axis, which is nominally maintained parallel to the orbit major axis.

The GPS experimental payload consists of two Trimble Advanced Navigation Sensor (TANS) Vector GPS receivers. The TANS Vector is a 6-channel, L1, C/A-code GPS receiver [9,13,14], which has been used for real time orbit and attitude determination applications in LEO. Each receiver has one master antenna and three slave antennas multiplexed on six receiver channels to measure differential carrier phase for determining host platform attitude. Code phase and Doppler from the master antenna are used for host platform position and velocity determination. The TANS Vector reports the following GPS observables: code phase, carrier phase, Doppler, and signal to noise ratio (SNR) measured through the master antenna, and differential phase and SNR measured through each of the three slave antennas. The receiver is capable of returning real-time position, velocity, clock, and attitude solutions when four or more satellites are tracked simultaneously.

Table 1: Nominal AO-40 Orbit

semimajor axis	36286 [km]
eccentricity	0.7968
inclination	6.04 [deg]
period	19.1 [hrs]
perigee altitude	1000 [km]
apogee altitude	58800 [km]

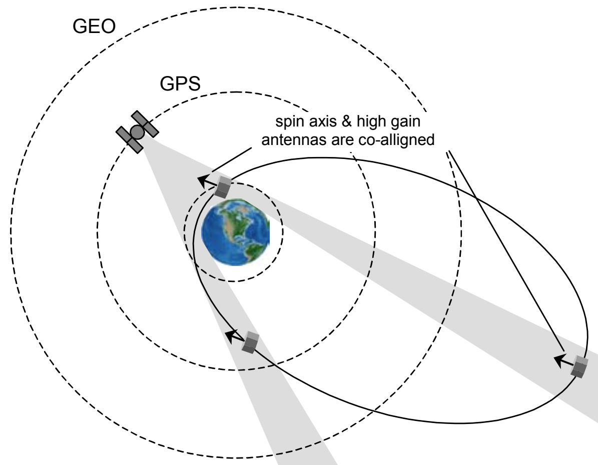

Figure 2: AO-40 orbit and spin axis orientation.

Two independent receivers were selected to provide redundancy and the capability to track GPS signals from antennas mounted on opposite sides of the spacecraft. Receiver 1 uses custom designed, two-stage pre-amplifiers connected to four high gain (approximately 10 dB) receiving antennas in order to compensate for the increased path losses expected at high altitudes. One of the high gain antennas is shown in Figure 3. The second GPS receiver is connected to four hemispherical patch antennas, intended to provide coverage at low altitudes near perigee.

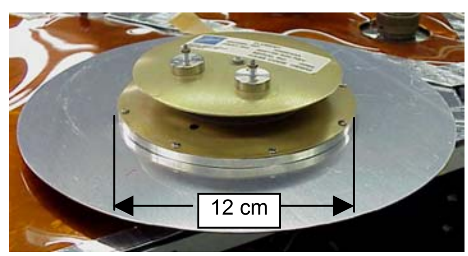

Figure 3: One of four high gain receiving antennas used with receiver 1.

The four high gain GPS antennas are shown mounted on the +Z face of the spacecraft in Figure 4. In this orientation, the antennas (and spin axis) point toward the center of the Earth (nadir) when the vehicle is at apogee, and towards zenith at perigee, providing favorable GPS coverage throughout the orbit (see Figure 2). The field of view of the each GPS antenna remains essentially fixed as the vehicle rotates, although other structures installed nearby begin to impinge on the field of view below 30-40 degrees elevation.

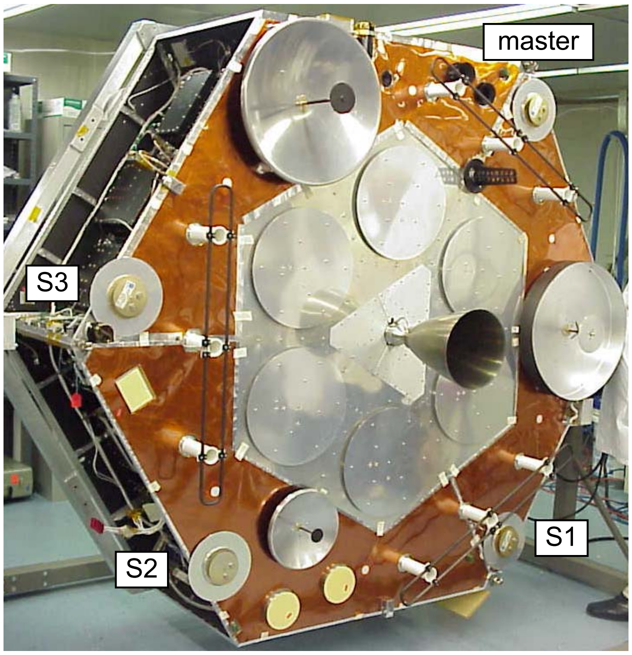

Figure 4: High gain GPS antennas (master, s1, s2, s3) mounted on the +Z spacecraft face.

Communication and control of the GPS and other experimental payloads on AO-40 is handled via the RUDAK (Regenerating Transponder for Digital Amateur Communications). The RUDAK is a pair of fully programmable computers each of which has its own error corrected memory and associated hardware modems and DSP modems [8]. The binary data from the GPS receivers are sent to the RUDAK via an RS-422 interface and binned into one-hour files that can be periodically downloaded to a suitably equipped ground station. Additional ground processing steps are performed to extract the individual measurement, status, and solution packets reported by the receiver.

EXPERIMENTAL RESULTS

This section highlights some of the most significant results from the AO-40 GPS experiment to date. Subsequent sections expand upon these results in greater detail.

Overview

Since September 2001, GPS Receiver 1, connected to the high gain antennas, has been operated for a total of 11 weeks from September 25 to November 2, 2001, and from May 11 to June 15, 2002. Although the TANS Vector was not originally designed to operate above the altitude of the GPS constellation, it has successfully tracked GPS satellites and returned measurements to the ground from vantage points throughout the orbit. Signal levels measured by the receiver were generally about 2 dB higher than predicted; the peak signal levels measured were approximately 48 dB-Hz when the spacecraft was at apogee (90000 km from the GPS satellite being tracked). The receiver typically lost lock at a signal level of approximately 42 dB-Hz, consistent with performance in ground tests.

The tracking performance described above was achieved while the spacecraft was spin-stabilized (5 RPM during the first data collection, 2.3 RPM during the second data collection). The spin of the vehicle introduces large amplitude variations in the received signals, and effectively reduces the field of view of the GPS antennas, because obstructions on the surface of the spacecraft pass through the field of view once per revolution (12 to 23 second period). Moreover, there was a noticeable adverse effect on the acquisition and tracking performance, particularly for signals received at low elevation angles near perigee. In some cases the receiver successfully acquired a signal, but the large variations in power levels caused intermittent tracking and prevented successful reception of the broadcast navigation message from that satellite. The amplitude variations were smallest when the line of sight to the GPS satellite was close to the receiving antenna boresite, and were larger for signals with larger off-boresite angles. Signals were generally not tracked more than 60 degrees off the receiving antenna boresite.

GPS signal levels measured by the receiver clearly indicate differences between the transmitted gain patterns of the earlier Block II/IIA GPS satellites, and the newer Block IIR vehicles. The receiver regularly (an average of once every few orbits) acquired and tracked side lobe signals. Most of the side lobe signals tracked were from Block IIR satellites, and the power levels were significantly higher than expected.

Earth-bound and near-Earth GPS receivers, including the TANS Vector, typically employ a satellite selection logic that presupposes a zenith pointing antenna attitude. This assumption is not valid for a receiver intended to track GPS signals across the limb of the Earth. The problem was addressed in previous HEO flight experiments by manually commanding the receiver to track specific satellites at pre-computed Doppler shifts. On AO-40, a simple "blind search" signal acquisition technique was used. Although this approach has significant limitations in terms of tracking signals near perigee (particularly for a six channel receiver), it allowed the receiver to operate continuously without requiring commanding from the ground, greatly increasing the amount of data returned.

Neither position nor attitude solutions were computed by the receiver in real time; however, there was one occasion during a perigee pass on October 5th when four satellites were tracked simultaneously allowing point solutions to be later computed on the ground. There were also several occasions when three satellites were tracked simultaneously. On a typical day, data outages lasting 1-4 hours, during which no satellites were tracked, were common.

The second GPS receiver, connected to the four patch antennas (on the opposite side of the spacecraft), was operated from June 15-19th. Unfortunately, as shown in Figure 2, the spacecraft attitude was unfavorable for GPS coverage through the patch antennas. During the short periods of time near perigee when strong GPS signals reach the antennas, much of the field of view is blocked by the Earth. Nevertheless, this receiver successfully tracked satellites during each perigee pass, with a maximum of three tracked simultaneously.

TRACKING PERFORMANCE AND MEASURED SIGNAL LEVELS

GPS Link Budget and Signal Visibility Model

The following parameters were estimated corresponding to the epochs of GPS measurements received from AO-40 for use in assessing the performance of the GPS experiment and analyzing the data returned:

- received carrier to noise spectral density, C/N_0
- vector line of sight, range, and Doppler
- limb crossing altitude (for evaluating ionosphere mask)
- estimated GPS satellite visibility, based on an assumed 42 dB-Hz tracking threshold for the TANS Vector
- off-boresite angles for the line of sight vectors with respect for the transmitting and receiving antennas, used to relate measured signal levels to antenna gain patterns

The models and assumptions used to compute the estimated GPS signal parameters are discussed in detail in [10], but are described briefly here.

Figure 5 illustrates the GPS signal reception geometry and variables modeled in the simulation. Since the receiver did not report position solutions, the AO-40 orbit is modeled based on NORAD two-line elements for the vehicle. The GPS satellite orbits are modeled based on GPS almanac data. The level of accuracy of these reference orbits (tens of kilometers) is sufficient to estimate GPS coverage and signal levels. The line of sight from the receiver to a single GPS satellite is computed as the difference between the position vector of the receiver and the position vector of the GPS satellite. The angle formed between the line of sight vector and the antenna boresite, **b**, is needed to map the measured signal levels to a corresponding antenna gain. Off-boresite angles for both the transmitting (α_t) and receiving (α_r) antennas, are computed from the estimated line of sight and the modeled orientation of the GPS satellite antenna and receiving antenna, respectively.

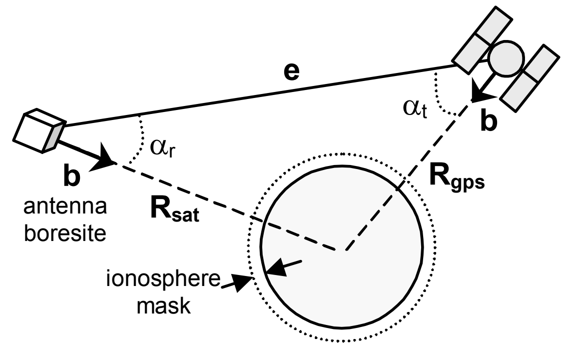

Figure 5: Modeled GPS signal geometry.

The transmitting antenna boresite of the GPS satellites is maintained within 0.5 degrees of the nadir direction (aligned with $\mathbf{R}_{gps}$). The boresite of the receiving antennas is nominally pointed towards the center of the Earth when the vehicle is at apogee, as shown in Figure 2. Telemetry from the spacecraft indicates the actual AO-40 attitude was within 3-4 degrees of the reference attitude during the 2002 data collection period discussed in this paper.

Estimated GPS satellite visibility is evaluated by determining when the line of sight from the receiver to GPS satellite is unobstructed (by the Earth or the local horizon) and the signal level is above the 42 dB-Hz tracking threshold of the receiver. The carrier to noise spectral density, C/N_0, of the signals was estimated by modeling the link budget between the GPS satellite and receiver, based on the assumptions listed in Table 2. Effective Isotropic Radiated Power from the GPS satellites was modeled at 30 dBW, or 3 dB above the level generally assumed to meet the minimum specified GPS power requirements for a user on the surface of the Earth [15]. The actual transmitted power varies by several dB over time, and from satellite to satellite.

The gain of the high gain receiving antennas was originally modeled based on a reference gain pattern supplied by the manufacturer. Unfortunately, the actual gain versus elevation response of the flight antennas mounted on the spacecraft was not measured prior to launch. Based on the flight data, the modeled gain pattern was later updated to more closely match the measured results, as discussed later in the paper. The GPS satellite antenna gain was modeled based on the mean gain pattern for a GPS Block II/IIA satellite from C. Czopek [11]. One of the objectives of the flight experiment was to evaluate how well this reference gain pattern matches the actual transmitted power levels from the GPS satellites.

Table 2: Link Budget Parameters/Assumptions

	Description	Assumption
EIRP	Effective Isotropic Radiated Power	30 [dBW]
G_t	gain of transmitting antenna in direction of **e**	see Figure 11
L_d	attenuation of signal with wavelength $\lambda = 0.1903$ m traveling a distance ρ	$20 \log \left(\frac{\lambda}{4\pi\rho}\right)$
G_r	gain of receiving antenna in direction of **e**	see Figure 12
T_{sys}	equivalent system noise temperature	190 [K]
L_{Nf}	noise figure of receiver/front end	-3.0 [dB]
L_I	implementation, A/D conversion losses	-1.5 [dB]

The estimated received power (at the input of the low noise amplifier) is computed from equation 1 by summing the transmitted power plus the modeled gain pattern of the GPS satellite, path losses, and gain of the receiving antenna,

$$\hat{P}_r = EIRP + G_t + L_D + G_r \qquad (1)$$

The estimated carrier to noise spectral density includes the estimated received power plus constant assumptions regarding the noise figure of the receiver and antennas, the system noise temperature, and implementation losses in the receiver,

$$C\hat{/}N_0 = \hat{P}_r - 10 \cdot \log_{10} T_{sys} + 228.6 + L_{Nf} + L_I \quad (2)$$

Measured versus Predicted GPS Tracking

Figure 6 shows an example of typical GPS tracking performance compared to the predictions for 24 hours on May 26, 2002. At high altitudes, the receiver successfully acquires and tracks most of the predicted GPS signal passes. The receiver has more difficulty near perigee due to the large Doppler shifts present. Operating in the blind search acquisition mode, the receiver is not necessarily searching for the correct satellites as they come into view. Also, satellites were usually only acquired as they passed

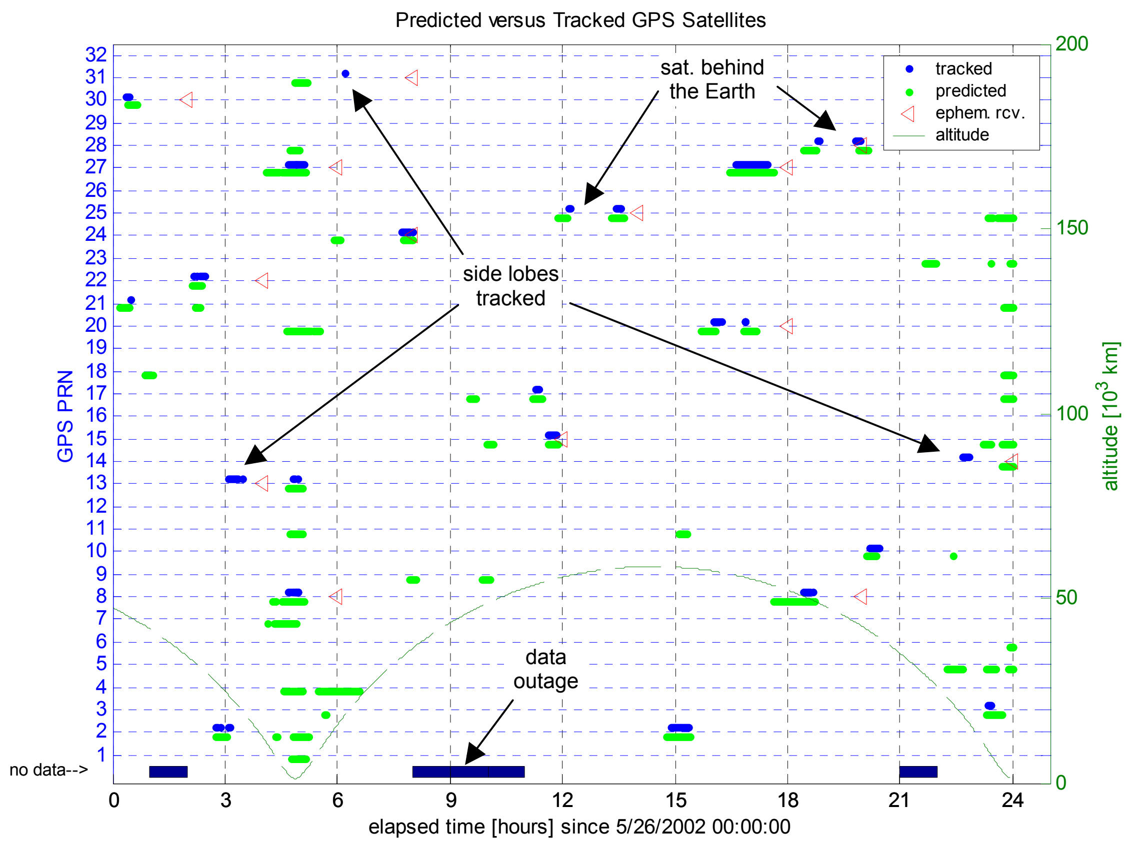

Figure 6: Actual versus predicted GPS tracking on May 26, 2002.

close to zero Doppler. Another factor contributing to the increased number of "missed" passes near perigee is an overly optimistic predicted visibility at low altitudes due to the assumption of a zero degree elevation mask when in fact the obstructions mounted near the GPS antennas impose an actual horizon mask of approximately 30 degrees as the vehicle spins.

During the first perigee pass around 05:00 hours, there were three satellites tracked simultaneously, but for the remainer of May 26, there were never more than 2 satellites tracked simultaneously. There are also three data outages indicated on the plot, in which no GPS data packets were downloaded from the receiver. It is assumed that no satellites were tracked during this time. In some cases pseudorange and Doppler measurements were returned for a GPS satellite but the receiver did not successfully decode the broadcast ephemeris data for that satellite. This is an indication that the receiver was having difficulty maintaining lock on the signal, and the satellite would not have been "usable" by the GPS receiver in a real-time solution.

The plot also shows three examples of tracked GPS side lobe signals. These passes were actually not predicted, as the signals were estimated to be below the tracking threshold of the receiver during this time.

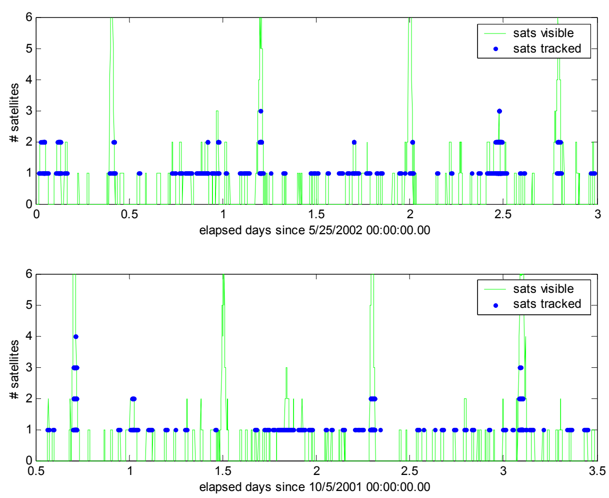

Figure 7: Number of satellites predicted versus tracked over two arcs from May 2002 and October 2001.

Figure 7 shows two longer examples of the number of satellites tracked over time; one between May 25-27, 2002, and the other between October 5-8, 2001. In the May example, there are two instances when three satellites were tracked simultaneously: during the perigee pass at approximately 1.2 elapsed days, and near apogee, at 2.5 elapsed days. The arc from October illustrates the only time when four satellites were tracked simultaneously during the perigee pass near 0.7 elapsed days. The receiver was not able to compute a solution at this time; however, because it only received valid ephemeris data for one of the four satellites.

Measured Signal Levels

The TANS Vector reports a signal to noise ratio measurement in Amplitude Measurement Units (AMU) from each antenna. The following expression is used to convert from AMU to a carrier to noise spectral density, C/N_0 expressed in dB-Hz,

$$C/N_0 = 10 \cdot \log_{10}(BW \cdot AMU^2) \qquad (3)$$

where BW is 1 kHz noise bandwidth associated with the receiver [13].

The spin stabilization employed for attitude control has a significant effect on the measured signal levels. Figure 8 shows an example of the measured signal levels from all four antennas on June 8, 2002 when the spacecraft was near apogee. The first plot spans one hour, while the second plot spans six minutes. The amplitude variations caused by the rotation of the vehicle are clear, and are correlated fairly well between the four antennas. The actual spin rate of the vehicle (5 RPM during the 2001 data collection, 2.3 RPM during the Spring 2002 data collection) can be seen in the period of the signal amplitude variations.

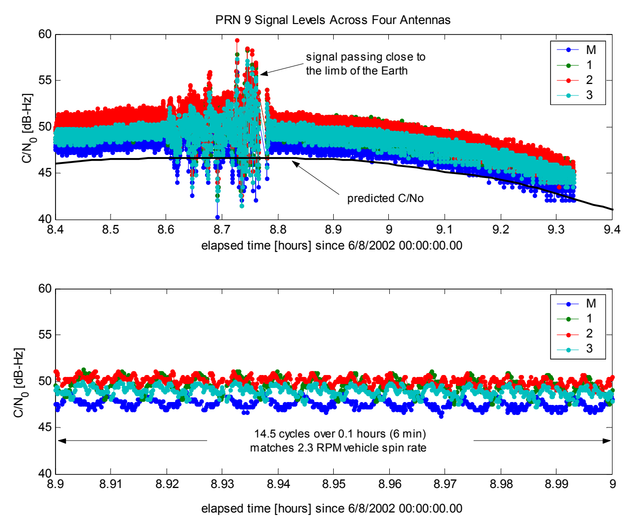

Figure 8: Comparison of signal levels measured from the master and three slave antennas. The top shows a one hour span. The bottom graph shows details over a 6 minute period. The oscillation in the measurements is due primarily to the spin of the vehicle.

The reported signal levels differed somewhat between the master and three slave antennas. Signal levels on slave antennas 1 and 2 were usually strongest (1-2 dB higher than the signals reported on the master antenna) and had slightly smaller peak-to-peak signal variations. The predicted C/N_0 for this satellite (also shown in Figure 8) is approximately 2 dB weaker than the mean measured signal level reported from the master antennas. This plot also provides an interesting example of the distortion caused by the ionosphere as the GPS signal passed very close to the limb of the Earth.

Figure 9 and Figure 10 provide examples of typical signal levels measured by the master antenna at apogee and perigee respectively, and comparisons with the predicted signal levels for these satellites. Peak signal levels at apogee were approximately 48 dB-Hz, while signals tracked through the high gain antennas near perigee were up to 60 dB-Hz. The differences between these peak levels are consistent with the expected 12 dB difference in path losses for a signal at apogee (-194.4 dB) versus a signal received near perigee (-182.4 dB). The peak measured signal levels were consistently 2 dB higher than predictions.

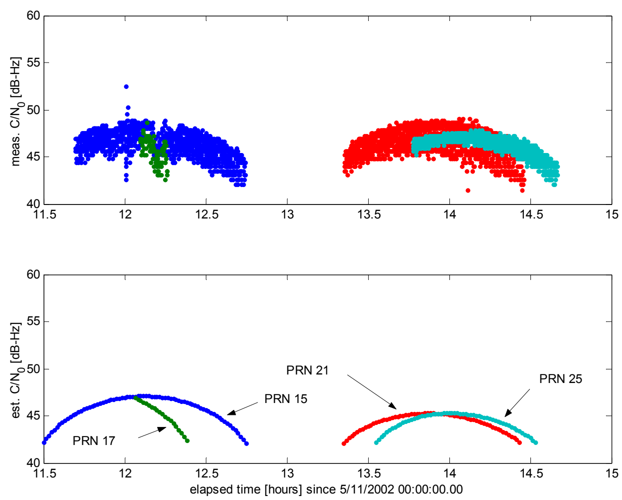

Figure 9: Typical signal levels measured by master antenna near apogee

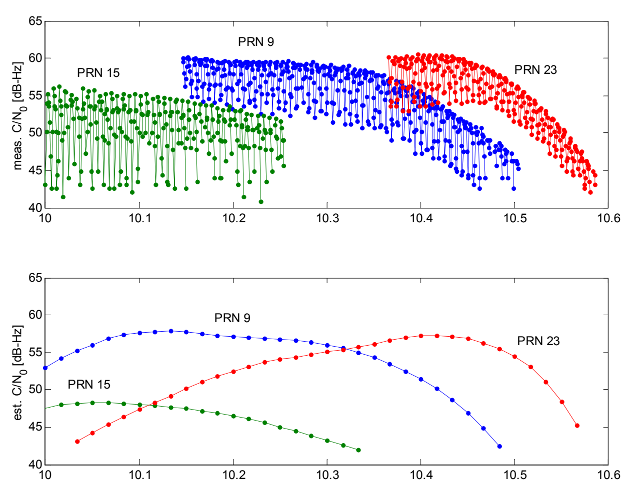

Figure 10: Typical signal levels measured by master antenna near perigee.

The large amplitude variations present in the measured signals are precisely correlated with the spin rate of the spacecraft. Peak-to-peak amplitudes ranged from 2 dB for signals tracked close to the boresite of the receiving antenna, to over 12 dB for larger received off-boresite angles. This phenomenon is caused because the actual gain from the receiving antenna is changing as the vehicle rotates, due to two factors:

1. The high gain antennas have a significant "squint," meaning that the gain pattern is not symmetrical in azimuth. This causes the measured C/No to vary as the antenna is rotated about the boresite. The effect is amplified for larger off boresite angles, as evidenced by the larger peak to peak signal oscillations for the signals tracked near perigee (up to 12 dB peak-to-peak in Figure 10).
2. A similar effect is caused if the actual spin axis of the spacecraft is offset slightly from the boresite of the GPS antenna. In this case, the actual boresite angle (and gain) of the received signal would vary as the vehicle rotates.

These two factors combine to make the signal levels reported by the receiver oscillate, although the effect of the antenna pattern asymmetry is greater than the contribution from spin axis misalignments. Furthermore, for low elevation signals (greater than 50-60 degrees off-boresite), objects mounted close to the antennas partially obscure the field of view. Signals with received off-boresite angles greater than 60 degrees were rarely tracked.

RECONSTRUCTION OF GPS SATELLITE TRANSMITTED POWER LEVELS

One of the primary objectives of the AO-40 GPS experiment was to return measurements of the GPS signal levels available for high altitude users. The specification on the transmitted signal levels from the GPS satellites is limited to 14.3 degrees off-nadir; the edge of the Earth plus 0.5 degrees for the maximum pointing error of the GPS satellites. There has long been some uncertainty as to the actual power levels transmitted at larger off-nadir angles, and how uniform these side lobe signals are. Furthermore, the gain patterns of the Block IIR satellites that began launching in 1997 are known to have a slightly narrower beamwidth than the earlier Block II/IIA satellites. Previous HEO flight experiments have yielded limited data to address these questions. Figure 11 shows a comparison between the assumed mean antenna gain patterns for the Block II/IIA and Block IIR satellites. The current 28 satellite GPS constellation consists of four of the oldest Block II vehicles (launched 1989-90), 18 of the Block IIA vehicles (launched 1990-97) and 6 of the newest Block IIR vehicles (launched since 1997).

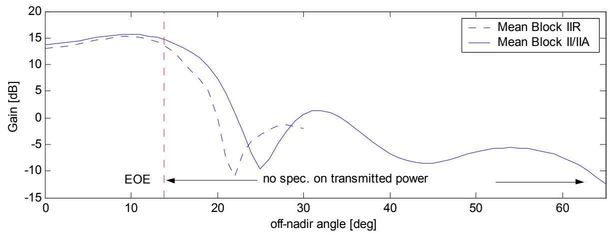

Figure 11: Mean gain patterns for the GPS Block II/IIA [11] and Block IIR [12] satellites.

By subtracting the known or estimated link budget parameters from the measured C/N_0, it is possible to reconstruct the "measured" gain pattern of the GPS satellites based on the measurements from AO-40. Because there is also some uncertainty as to the shape of the receiving antenna gain patterns, an iterative process was used. Re-arranging equations 1 and 2, and grouping all of the constant terms, the predicted C/N_0 consists of three time varying components (gain of the transmitting antenna along the line of sight, path losses, and gain from the receiving antenna) plus a constant signal offset,

$$C\hat{/}N_0 = G_t + L_D + G_r + c \qquad (4)$$

Substituting the measured C/N_0 from equation 3 and solving for G_t results in an expression for the measured gain of the GPS transmitter,

$$G_t = C/N_0 - \hat{L}_D - \hat{G}_r - c \qquad (5)$$

Since the actual gain versus elevation response of the receiving antennas flown on AO-40 is not known, rearranging equation 5 to solve for G_r provides a way to compute the "measured" gain of the receiving antennas,

$$G_r = C/N_0 - \hat{L}_D - \hat{G}_t - c \qquad (6)$$

The following procedure was used to reconstruct the transmitted signal levels from the AO-40 GPS measurements:

- Signal to noise measurements reported by the master antenna were averaged to remove the oscillations induced by the rotation of the vehicle. The equivalent "mean C/N_0" was then computed using equation 3.
- Expected C/N_0, off-nadir angle (α_t), and received off-boresite angle (α_r) were computed corresponding to the measurements.
- Using only signals transmitted from the most uniform region of the GPS satellite antenna array (0-15 degrees off-nadir), and not falling within a 500 km ionosphere mask, a composite plot of the signal levels versus received off-boresite angle was generated (Figure 12). This "measured" elevation versus gain response was used to update the model for the receiving antenna.
- Estimated signal levels were recomputed using the new receiving antenna pattern. Measurements within 0-25 degrees of the receiving antenna boresite and outside the 500 km ionosphere mask were used to create a composite plot of the signal levels versus the transmitter off-nadir angle (Figure 13, Figure 14). This is the "measured" gain pattern of the GPS satellites.

The measured gain of the receiving antenna was computed from equation 6 and plotted versus the estimated off-boresite angle in Figure 12. This plot was constructed by compiling the mean GPS signal levels measured from May 14 to June 15, 2002. It also shows the original modeled attenuation pattern provided from the manufacturer and the updated pattern derived from the measurements, which has been used in subsequent analysis. Selecting only those measurements transmitted from the most uniform regions of the GPS satellite attenuation pattern minimized the contribution of errors due to mismodeling of the GPS satellite power levels in this plot.

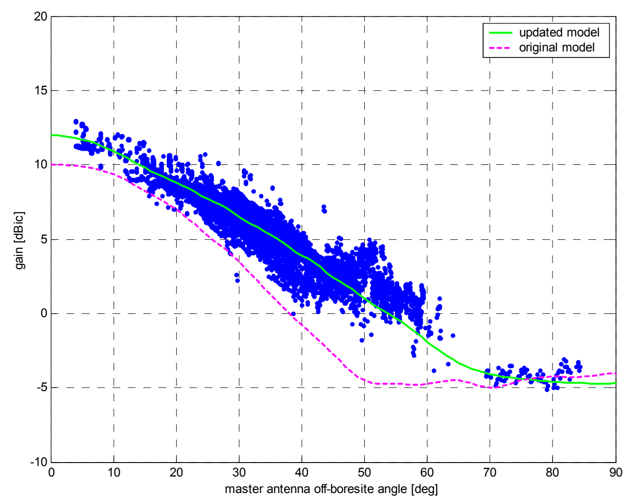

Figure 12: Gain pattern of the master receiving antenna derived from signal to noise measurements recorded between May 14 and June 15, 2002.

As mentioned in the previous section, Figure 12 again illustrates a 2 dB difference between the measured versus estimated signal levels. This implies that the sum of the constant c plus the modeled gain of the transmitting and receiving antennas is about 2 dB conservative with respect to the mean measured signals. In this plot, it shows up as a positive offset in the measured value of G_r, but does not change the actual shape of the antenna pattern derived from the measured signal levels. In the updated link analysis used to reconstruct the GPS satellite gain patterns, the peak received gain was increased by 2, to 12 dB, to correspond to the measured gain indicated in Figure 12.

The measured gain of the GPS satellite transmitting antennas, shown in Figure 13, was constructed from equation 5 using the signal to noise ratio measurements recorded between May 11 and June 15, 2002. The data was normalized to 0 dB at the edge of the Earth. The updated model for the receiving antenna was used. The majority of side lobe signals tracked are from Block IIR satellites, and are radiated between 50 to 60 degrees off-nadir. The small number of side lobe measurements from block II/IIA satellites are of similar amplitude and were transmitted from within the same region. Since the measured side lobe signals were significantly higher than expected, additional checks were performed to verify these signals were actually interpreted correctly as side lobes. This was done by examining the altitude of the AO-40 spacecraft and range to the GPS satellites when the side lobes were tracked, and by comparing the predicted versus measured Doppler shifts of the side lobe signals. It is important to note that the actual transmitted side lobes at a constant off-nadir angle may vary significantly as the GPS transmitter is rotated in azimuth, or between different GPS satellites, so these signal levels are not necessarily available at all times.

Figure 14 shows the measured versus predicted GPS main lobe signals, constructed using a subset of the signal to noise levels measured from within 25 degrees of the receiving antenna boresite. Imposing this mask angle on the receiving antenna removes the noisiest data and helps to minimize the effects of the spin-induced signal variations. The shape of the measured GPS satellite antenna pattern agrees very well with the predicted pattern within the specified region between 0-14.3 degrees off-nadir. Beyond 14.3 degrees, there is no specification on the antenna pattern or transmitted signal levels; however, the expected difference in shape between the mean Block II/IIA and block IIR antenna patterns is clearly evident in this region.

The largest errors in the reconstruction of the GPS satellite antenna patterns (equation 5) are due to the spin-induced oscillations in the received signal levels and uncertainty in the actual gain patterns of the transmitting and receiving antennas. The adverse effects of the spin-stabilization are minimized by averaging the raw signal to noise levels. Furthermore, by using transmitter data only from signals that are near the boresite of the GPS satellites, we have minimized the effect of this uncertainty in compiling the measured receiver antenna pattern, and conversely, by using data along the receiver boresite only, we hope to minimize errors in reconstructing the GPS transmission patterns. These modeling errors plus satellite-to-satellite power variations between the GPS satellites cause a distribution of measured signal levels. When all the signal to noise measurements are considered (Figure 13), the measured gain variations were always less than 5-7 dB. Excluding measurements subject to the largest modeling errors reduces the peak measured signal differences to 4-5 dB in Figure 14.

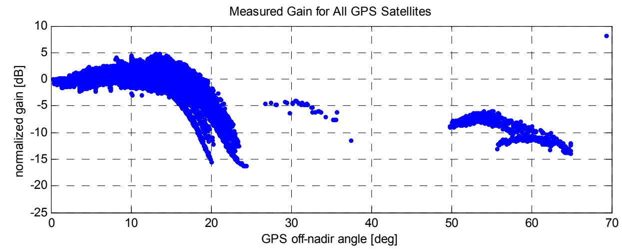

Figure 13: The measured gain pattern of the GPS satellites reconstructed from signal to noise ratio measurements made between 11 May to 15 June 2002.

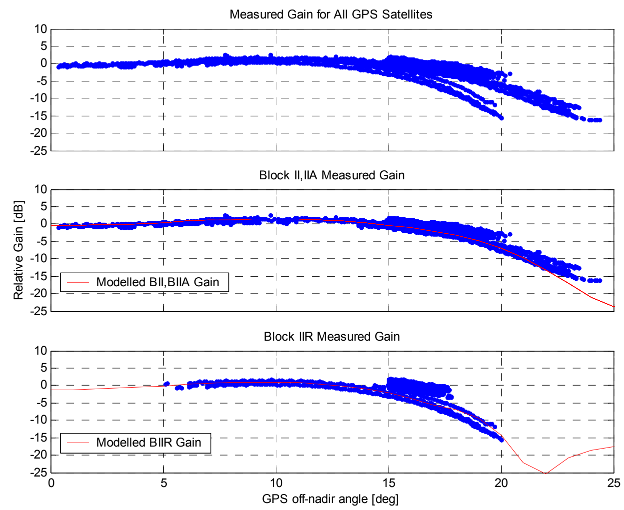

Figure 14: The measured gain pattern of the GPS satellites reconstructed from a subset of the signal to noise measurements. The first plot shows the signals for all of the satellites; the second plot only the block II/IIA satellites; and the third plot only the block IIR satellites. The data is normalized to zero dB at 14.3 degrees off-nadir, (edge of the Earth for the worst case satellite off-axis angle of 0.5 degrees).

CHALLENGES FACED BY A GPS RECEIVER IN HEO

The AO-40 GPS experiment has yielded a number of useful insights into the challenges associated with operating a GPS receiver in a HEO; furthermore, it has highlighted a number of limitations in the TANS Vector (and many other conventional GPS receivers) that limit their applicability for such an orbit.

One of the most significant problems with the GPS measurements reported from AO-40 was the lack of any knowledge of the behavior of the receiver clock. Since solutions were never performed by the receiver in real time, the bias in the local clock, subsequently inherent in the measurements and time tags, is unknown. This problem is exacerbated because in the absence of a solution for long periods of time, the receiver periodically (erroneously) shifts the local clock by hundreds of milliseconds based on information contained in the HOW bits of the broadcast navigation message from the GPS satellites. The precise magnitude and frequency of these clock adjustments are unknown.

The problem is caused by another common assumption employed in many GPS receivers. When a receiver is powered on, the local time, t_r, is set approximately based on t_{HOW}, the time derived from information embedded in the hand-over-word bits of the broadcast navigation message from the first satellite tracked,

$$t_r = t_{HOW} + d \qquad (7)$$

Later, after four satellites have been acquired, the local clock is set precisely (within ~100 ns) based on the receiver's clock bias solution. The variable d in equation 7 is usually set to a constant value corresponding to the typical path delay to the GPS satellites, approximately 0.07 seconds for a terrestrial or LEO user. Ground-based tests revealed that the TANS Vector routinely sets its clock to within ±10ms of GPS time using this method when operated in a LEO, a level of error consistent with the actual range of propagation delays expected for a LEO user.

The range of propagation delays experienced by a receiver in a HEO is much larger. The actual signal delay to a GPS satellite from within the AO-40 orbit can be up to 0.300 seconds (300 ms) for satellites tracked near apogee. Unfortunately, in the absence of a solution, the receiver continually checks the local clock against t_{HOW} each time a new satellite is acquired. Even if the clock was set precisely near apogee, the first time a satellite is tracked across the limb of the Earth, a clock error of approximately 100 ms is introduced. The receiver makes these adjustments multiple times each orbit, unfortunately no information is available about their actual magnitude or frequency. An illustration of the assumed behavior is shown in Figure 15. The discontinuities in the receiver clock make it difficult to recover the actual clock behavior by processing the measurements. Furthermore, double differencing techniques that could be employed to remove the receiver clock error are only feasible during the limited occasions when two or more satellites were tracked simultaneously.

The problems related to the clock behavior are further complicated because the "code phase" reported by the TANS Vector does not include all of the information normally contained in a full pseudorange measurement. The pseudorange observation between a receiver and GPS satellite is formed by measuring the observed signal propagation delay scaled by the speed of light, shown on the left side of equation 8,

$$\rho = c\left(t_r - t_{gps}\right) = \left|\mathbf{r}_{gps} - \mathbf{r}_{\mathbf{r}}\right| + c \cdot b_r + \varepsilon \qquad (8)$$

The pseudorange observable is related to the user position and clock states by the right half of equation 8, where $\mathbf{r}_{\mathbf{gps}}$ is the position of the GPS satellite at transmit time; $\mathbf{r}_{\mathbf{r}}$ is receiver position at receive time; b_r is the bias in the receiver clock in seconds; and ε is the composite of GPS satellite clock bias, GPS ephemeris mis-modeling, other error sources.

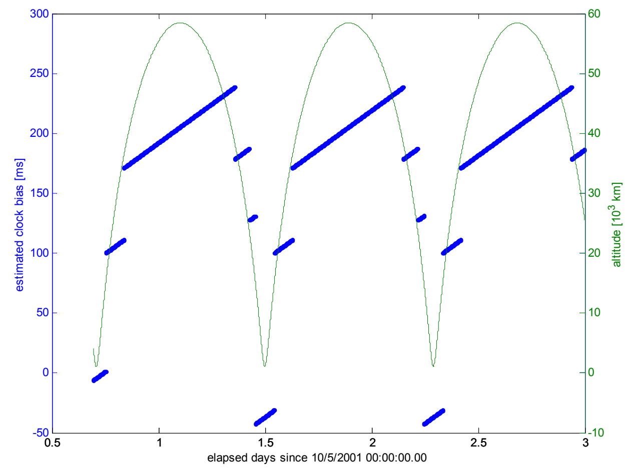

Figure 15: Simulated behavior of the TANS Vector clock in the AO-40 orbit based on a clock drift of 450 m/s.

A significant component of the pseudorange measurement is the actual bias in the local receiver time, t_r. In the case of AO-40, the true range is consistent with a propagation delay of anywhere from 70 to 300 ms; however, the clock bias can be of similar magnitude (Figure 15). The code phase measurement reported by the TANS Vector is a modulo 1 ms (or ~293 km) number, essentially the fractional component of the pseudorange. This is a compact way of reporting the pseudorange, assuming the actual local clock error never exceeds 0.5 ms; a condition normally satisfied when the receiver is computing solutions. Unfortunately, there is no way to directly recover the integer millisecond component of the actual clock bias, which can be hundreds of milliseconds, from only the code phase measurement.

Two additional minor issues specific to the TANS Vector are related to the raw measurements available from the receiver. The raw code phase and Doppler measurements are not synchronous and are not coincident with the carrier phase measurements. This implies that the code phase and Doppler measurements must be interpolated to the carrier phase time tags in order to produce data in the "standard" RINEX format required as an input to a variety of GPS data processing tools. Additionally, the signal levels from the TANS Vector are reported using a proprietary amplitude measurement scale that can only be approximately related to the more commonly used carrier to noise spectral density in dB-Hz.

GPS-BASED ORBIT DETERMINATION

Some level of success has been achieved from attempts to process the raw measurements from the GPS receiver using both batch and sequential filtering techniques. Unfortunately, there is very limited ground-based tracking data available for the AO-40 spacecraft, so the best reference trajectories available are assumed to be accurate only to tens of kilometers. Also, as described in the previous section, the receiver does not report full pseudoranges, and since it has yet to compute a point solution onboard, an unambiguous clock bias has not yet been determined. The receiver's clock maintenance strategy, in which it resets its clock in a non-deterministic fashion when there are long outages, further complicates the problem.

Preliminary batch orbit determination results from AO-40 are described in detail in Davis et al [7]. In an onboard embedded OD application, a sequential filter processes the measurements in real time. Several sequential filtering studies using simulated HEO data have been performed [16], but AO-40 offers the first opportunity to calibrate these simulation results against flight data. To this end, four days of data taken from October 5, 2001 through October 9, 2001 were processed using the GPS-Enhanced Onboard Navigation System (GEONS) [17]. The pseudo-ranges were reconstructed using the NORAD TLEs and zero clock bias and rate values via the process described in Davis et al. [7].

On October 5, there were 12 observation times that had four GPS PRNs visible spanning 223 seconds. The 12 observations were processed using a stand-alone point solution utility. The position difference between the point solutions and the TLE-based reference orbit was between 115 and 123 kilometers. The 12 point solutions were processed as measurements in the Goddard Trajectory Determination System (GTDS), a high-fidelity batch orbit determination (OD) processor that is used for mission operations [18]. The resulting measurement residuals varied from -140 to 180 meters. The position differences between an ephemeris derived from the GTDS solution and the TLE-based reference orbit varied from 9.2 to 125 kilometers. These results are consistent with Davis et al [7].

GEONS was initialized with the GTDS epoch solution, and using the point solution clock bias and clock rate. The reconstructed pseudorange data weight was 15 meters, and GPS signal paths within 500 km of the earth limb were excluded. As Figure 16 shows, the resulting GEONS solutions are consistent with the GTDS ephemeris, with a worst-case error better than 25 km. These results should not be taken as definitive, largely because of the unknown clock bias present both in the TANS pseudoranges and their time tags, which affects both the GEONS results and the GTDS ephemeris to which they are compared. Only if receiver-generated point solutions that contain the full clock bias become available will it be possible to fully validate previous studies of onboard GPS OD.

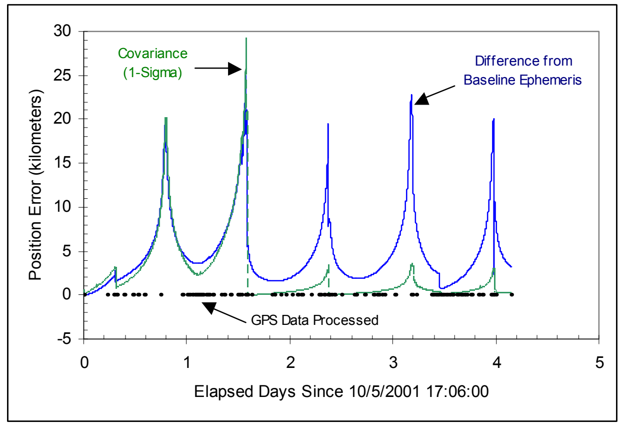

Figure 16: Total position error between GEONS solution and GTDS ephemeris reference. GEONS processing with covariance of 316 m and 1 m/s, and initial position and velocity state errors of 100 m and 0.100 m/s each axis.

SUMMARY

A GPS receiver flying in a 1000 by 59,000 km altitude orbit has been returning GPS observations from high above the altitude of the GPS constellation. This experiment has succeeded in autonomously operating a low-cost GPS receiver in a HEO, further validating GPS-based navigation as a viable concept onboard spacecraft reaching very high altitudes. Signal to noise levels as high as 48 dB-Hz were measured near apogee, when the vehicle was at an altitude of 60000 km (approximately 10 R_E), indicating that with a suitable RF design and antenna, GPS signals could be successfully tracked significantly higher. GPS side lobe signals were tracked on several occasions, primarily from the newer, Block IIR GPS satellites. The signal level measurements have been used to reconstruct the transmitted power levels from the GPS satellites and obtain a better understanding of the signals available to high altitude users. This performance is more impressive considering the spin stabilization employed for attitude control reduces the field of view of the receiving antennas and adversely affects the tracking performance of the receiver.

The receiver has not computed a solution in real time; however, GPS measurements have been processed using batch and sequential filtering techniques. The GPS orbit determination results compare to the available reference trajectories to within tens of kilometers, unfortunately, the uncertainty in the reference trajectory is at the same level. The experiment has provided important operational experience dealing with the many challenges inherent to GPS tracking at high altitudes. Several limitations in the GPS receiver have come to light, reinforcing the argument that many aspects of the GPS receiver design must be carefully considered before flying in a HEO. The implications of this experiment are, despite the challenges, that GPS-based orbit determination using a well-designed receiver is a viable option for a wide variety of HEO spacecraft.

ACKNOWLEDGEMENTS

The authors would like to acknowledge the AMSAT organization whose dedicated members have made this experiment possible. Bdale Garbee supported the integration of the GPS experiment as the AMSAT GPS project manager. Most recently, Jim White and Mike Kingery, spent many hours (sometimes during the middle of the night) downloading the GPS data from the RUDAK via their personal ground stations. Larry Jackson and Charles Campbell at NASA GSFC developed procedures and software to decode the binary data from the RUDAK and convert to the ASCII TANS Vector measurement packets. Anne Long and Taesul Lee of Computer Sciences Corporation assisted in the efforts to process the GPS data from the receiver in GEONS. Finally, Glenn Lightsey of the University of Texas was instrumental in making some key modifications to the satellite selection algorithms in the TANS Vector, without which the receiver would not have been capable of operation above the GPS constellation.

REFERENCES

1. Bauer, F., et al., “Spaceborne GPS: Current Status and Future Visions,” *Proceedings of the Institute of Navigation GPS 1998 Conference*, Nashville, TN, September 1998, pp. 1493-1508.
2. ESTEC, *TEAMSAT Results*, April 21, 1998, <http://www.estec.esa.nl/teamsat/page_menu_results.html>.
3. Balbach, O., et al., "Tracking GPS Above GPS Satellite Altitude: First Results of the GPS Experiment on the HEO Mission Equator-S," *IEEE PLANS*, 1998, pp. 243-249.
4. Powell, T.D., P. D. Martzen, S.B. Sedlacek, C. Chao, R. Silva, A. Brown, G. Belle, “GPS Signals in a Geosynchronous Transfer Orbit: Falcon Gold Data Processing,” ION Nation Technical Meeting, January, 1999, pp. 575-585.
5. Kronman, J.D., “Experience Using GPS for Orbit Determination of a Geosynchronous Satellite,” *Proceedings of the Institute of Navigation GPS 2000 Conference*, Salt Lake City, UT, September 2000.
6. M.C. Moreau, F. Bauer, J.R. Carpenter, E. Davis, G. Davis, L. Jackson, “Preliminary Results of the GPS Flight Experiment on the High Earth Orbit AMSAT OSCAR 40 Spacecraft," 25th Annual AAS Guidance and Control Conference, Breckenridge, CO, February 6-10, 2002.
7. G. Davis, M. Moreau, F. Bauer, J.R. Carpenter, “GPS Based Navigation and Orbit Determination for the AMSAT AO-40 Satellite," AIAA Guidance and Control Conference, Monterey, CA, Aug 2002.
8. Williamson, P., *The Radio Amateur Satellite Corporation*, Last Updated: August 11, 2002, <http://www.amsat.org/>.
9. Trimble Navigation Limited, *TANS VECTOR Specification and User’s Manual*, May, 1995.
10. M.C. Moreau, *GPS Receiver Architecture for Autonomous Navigation in High Earth Orbits*, Ph.D. Dissertation, Department of Aerospace Engineering Sciences, University of Colorado at Boulder, July 2001.
11. Czopek, F., "Description and Performance of the GPS Block I and II L-Band Antenna and Link Budget," *Proceedings of the Institute of Navigation GPS 93 Conference*, pp. 37-43.
12. Personal communication with T. Powell, Aerospace Corporation, September 2002.
13. Cohen, C.E., *Attitude Determination Using GPS*, Ph.D. Dissertation, Department of Aeronautics and Astronautics, Stanford University, December, 1992.
14. Lightsey, E.G., *Development and Flight Demonstration of a GPS Receiver for Space*, Ph.D. Dissertation, Department of Aeronautics and Astronautics, Stanford University, February 1997.
15. Ward, P., “GPS Satellite Signal Characteristics,” Chapter 4 in E. Kaplan (editor), *Understanding GPS: Principles and Applications*, Artech House Publishers, 1996.
16. Moreau, M.C., P. Axelrad, J.L. Garrison, A. Long, “GPS Receiver Architecture and Expected Performance for Autonomous Navigation in High Earth Orbits,” *Navigation*, Vol. 47, No. 3, Fall 2000, pp. 191-204.
17. Goddard Space Flight Center, Flight Dynamics Division, CSC-5506-06R0UD0, *Global Positioning System (GPS) Enhanced Orbit Navigation System (GEONS) System Description and User’s Guide,* Version 1, Release 1.2, prepared by Computer Sciences Corporation, July 2002.
18. Goddard Space Flight Center, FDD/552-89/01, *Goddard Trajectory Determination System (GTDS) Mathematical Theory Revision 1,* A. Long et al.NASA Goddard Space Flight Center, June 1989.